

## Study on the change in properties of uranium dioxide by co-doping of trivalent and tetravalent elements

Jeongmook Lee<sup>a\*</sup>, Hye Ran Noh<sup>a,b</sup>, Hyun Myung Choe<sup>a,c</sup>, Dong Woo Lee<sup>a</sup>, Jong-Yun Kim<sup>a,b</sup> and Sang Ho Lim<sup>a,b</sup>

<sup>a</sup>Nuclear Chemistry Research Team, Korea Atomic Energy Research Institute, 111 Daedeok-daero 989 Beon-gil, Yuseong-gu, Daejeon, 34057, Republic of Korea

<sup>b</sup>Department of Radiochemistry & Nuclear Nonproliferation, University of Science & Technology, Gajeong-ro 217, Yuseong-gu, Daejeon, 34113, Republic of Korea

<sup>c</sup>Department of Chemistry, Sogang University, Baekbeom-ro 35, Mapo-gu, Seoul, 04107, Republic of Korea

\*Corresponding author: leejm@kaeri.re.kr

### 1. Introduction

After irradiation of  $\text{UO}_2$  nuclear fuel in the reactor, fission products (FPs), lanthanides (Ln), actinides (An) and activation products are produced and located in the fuel [1-3]. Those elements are doped in the nuclear fuel as  $(\text{U,FP,Ln,An})\text{O}_{2\pm x}$  form. To understand the structural character of the spent nuclear fuel, element doped  $\text{UO}_2$  have been studied as simulated spent fuel. The element doping effect has influence on the phase stability in U-FP/Ln/An-O system, thermal conductivity and the relevant fuel performance. Raman spectroscopy has been used to investigate surface structure of the nuclear fuel materials, because of its sensitivity, convenience and non-destructive sample preparation [4]. The Raman studies on trivalent-doped  $\text{UO}_2$  directly show the defect due to oxygen vacancy that could be created by loss of oxygen for charge compensation [5- 7]. This defect has significant effect on the kinetics of fuel oxidation. Previous studies have been focused on single element doped  $\text{UO}_2$ . In this study, we have been investigated the effect on both Gd-and Zr-doping on the  $\text{UO}_2$  structure with various experimental techniques to characterize the influence of co-doping of trivalent and tetravalent elements.

### 2. Experimental Section

$\text{U}_{1-x-y}\text{Gd}_x\text{Zr}_y\text{O}_2$  ( $x=0, y=0; x=0.005, y=0.05; x=0.005, y=0.1; x=0.01, y=0.05$ ) pellets were prepared by using a powder mixing method. The pellets were sintered at 1700 °C for 18 h and then cooled to room temperature in a reducing atmosphere with hydrogen gas.

Scanning electron microscopy (SEM, Jeol, USA) results revealed morphological and dispersive features of Gd and Zr in  $\text{UO}_2$ . X-ray diffraction (XRD) patterns of samples were performed with a Bruker AXS D8 Advance X-ray Diffractometer using  $\text{Cu K}\alpha$  radiation. The Raman spectroscopy was measured with an ANDOR Shamrock SR500i spectrometer, using a He-Ne laser with a wavelength 632.8 nm. Electrical conductivities of pellets were determined by calculating specific resistivities analyzed with 4- point probe (HM21-Jandel Co., UK).

To study the electrochemical behaviors of samples,  $\text{U}_{1-x-y}\text{Gd}_x\text{Zr}_y\text{O}_2$  electrodes were prepared mounting pellets onto steel-working electrode. And 3 electrode system (CHI-600D, USA) is used for cyclic voltammetry and RDE system of 1000 rpm (PINE, USA) in carbonate/bicarbonate dissolved in 0.1 M NaCl solution ( $[\text{HCO}_3^-/\text{CO}_3^{2-}]=0.01 \text{ mol L}^{-1}$ ). All electrodes were polished with sand papers of 1000 grid before electrochemical analyses.

### 3. Results & Discussion

In case of  $\text{UO}_2$  sample has polygonal structures consisted of wrinkled and flattened domains. It is also observed that the domain size decreases rapidly with increase of Gd and Zr doping level.

XRD patterns of all samples show similar features each other (Fig. 1). The lattice parameters are refined from each XRD spectrum and they show linearly decreasing of lattice change with increasing doping level. Because  $\text{Gd}^{3+}$  (1.053 Å) and  $\text{Zr}^{4+}$  (0.84 Å) have difference ionic radii than  $\text{U}^{4+}$  (1.001 Å), the lattice parameter decreases with increasing doping level. The portion of  $\text{Zr}^{4+}$  is higher than that of  $\text{Gd}^{3+}$  for all doped samples.

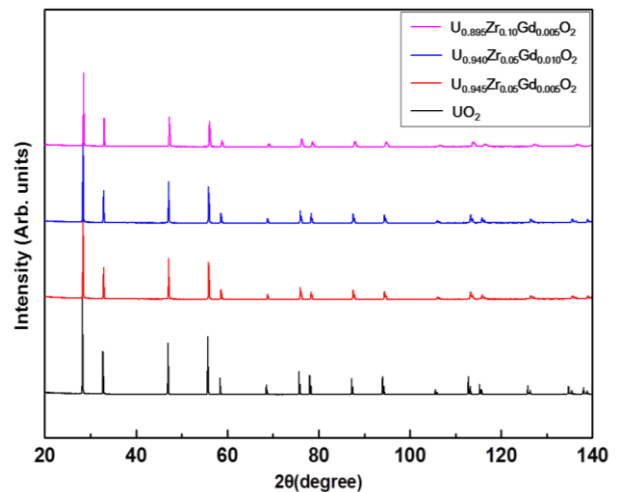


Fig. 1. Raman spectra of  $\text{UO}_2$  (up, black line) and  $\text{U}_{1-x-y}\text{Gd}_x\text{Zr}_y\text{O}_2$  (bottom, colored lines) pellets

Raman spectra of all samples show significant two peaks at  $\sim 445$  and  $\sim 1150 \text{ cm}^{-1}$  that were assigned to U-

O symmetric stretching mode in the fluorite structure [14-16] and an overtone of the first order longitudinal optical (L-O) phonon mode regarded as fingerprint for quasi-perfect fluorite structure, respectively. For doped samples, the intensities of two peaks at  $\sim 445$  and  $\sim 1150$   $\text{cm}^{-1}$  markedly decrease, but the broad band in the region 500 to 650  $\text{cm}^{-1}$  increase. The decreasing intensity of peaks at  $\sim 445$  and  $\sim 1150$   $\text{cm}^{-1}$  means the lattice distortion of perfect fluorite structure. The broad band was deconvoluted to three peaks at  $\sim 530$ ,  $\sim 575$ ,  $\sim 600$  and  $\sim 630$   $\text{cm}^{-1}$ . The peaks at  $\sim 530$ ,  $\sim 575$  and  $\sim 630$   $\text{cm}^{-1}$  were ascribed as defect due to oxygen vacancy associated with  $\text{Gd}^{3+}$ , first order L-O phonon mode due to crystal lattice disorder and formation of  $\text{M}_4\text{O}_9$ , respectively. The peaks at  $\sim 530$ ,  $\sim 575$  and  $\sim 630$   $\text{cm}^{-1}$  were assigned as  $\text{ZrO}_8$ -type complex forms in the fluorite  $\text{UO}_2$  matrix via successive accommodation of doped Zr. The relative area ratios of each peak to the peak at  $\sim 445$   $\text{cm}^{-1}$ , give qualitative information about formation of each lattice disorder.

Electrical conductivities, obtained from measuring the specific resistivity of each pellets, increased as increasing doping level. However there is no clear trend.

Cyclic voltametric experiments were done to determine the susceptibility to anodic oxidation. It has been known that Gd-doping suppresses both stages of anodic oxidation; matrix oxidation ( $\text{UO}_2 \rightarrow \text{UO}_{2+x}$ ) and its further oxidation to soluble  $\text{U}^{6+}$  (as  $\text{UO}_2^{2+}$ ). Our samples, both Gd and Zr doped, show similar results.

#### 4. Conclusions

$\text{U}_{1-x-y}\text{Gd}_x\text{Zr}_y\text{O}_2$  pellets have been characterized by SEM, XRD, Raman spectroscopy, electrical conductivity and electrochemical experiment. The substitution of Gd and Zr atoms into the  $\text{UO}_2$  lattice is confirmed by lattice parameters from XRD spectra. Raman spectra show that presence of  $\text{Gd}^{3+}$ -oxygen vacancy clusters and  $\text{ZrO}_8$ -type complex in the structure of  $\text{U}_{1-x-y}\text{Gd}_x\text{Zr}_y\text{O}_2$ . Electrochemical experimental results also show the influence of Gd-and Zr-doping on kinetics of oxidation.

#### REFERENCES

- [1] H. Kleykamp, The chemical state of the fission products in oxide fuels, *Journal of Nuclear Materials*, Vol.131, pp. 221-246, 1985.
- [2] R.J.M. Konings, T. Wiss, O. Beneš, Predicting material release during a nuclear reactor accident, *Nature Materials*, Vol.14, pp. 247-252, 2015.
- [3] R.C. Ewing, Long-term storage of spent nuclear fuel, *Nature Materials*, Vol.14, pp. 252-257, 2015.
- [4] M. Schmitt, J. Popp, Raman spectroscopy at the beginning of the twenty-first century, *Journal of Raman Spectroscopy*, Vol.37, pp. 20-28, 2006.
- [5] L. Desgranges, Y. Pontillon, P. Matheron, M. Marcet, P. Simon, G. Guimbretie, et al., Miscibility Gap in the U-Nd-O Phase Diagram: a New Approach of Nuclear Oxides in the

Environment?, *Inorganic Chemistry*, Vol.51, pp. 9147-9149, 2012.

[6] Z. Talip, T. Wiss, P.E. Raison, J. Paillier, D. Manara, J. Somers, et al., Raman and X-ray Studies of UraniumLanthanum-Mixed Oxides Before and After Air Oxidation, *Journal of American Ceramic Society*, Vol.98, pp. 2278-2285, 2015.

[7] F. Lebreton, D. Horlait, R. Caraballo, P.M. Martin, A.C. Scheinost, A. Rossberg, et al., Peculiar Behavior of (U,Am)O<sub>2</sub>- $\delta$  Compounds for High Americium Contents Evidenced by XRD, XAS, and Raman Spectroscopy, *Inorganic Chemistry*, Vol.54, pp. 9749-9760, 2015